AGU ADVANCING EARTH AND SPACE SCIENCES

Justin T. Maxwell, Shelly Rayback
Investigation: Grant L. Harley, Justin T. Maxwell, Edward Cook, R. Stockton Maxwell, Maegen L. Rochner, Ellen V. Bergan, Zachary Foley, Matthew Therrell, Joshua Bregy
Methodology: Edward Cook

RESEARCH LETTER
Geophysical Research Letters
10.1029/2024GL109099

Key Points:

- Maximum latewood blue intensity from tree rings can effectively be used to develop paleotemperature estimates for the southeastern US
- The fidelity of tree-ring density parameters for paleoclimate reconstruction are influenced by disturbance regimes and microsite conditions
- Compared to the last 260 years, regional 20th-century maximum late summer temperatures are not characterized by unprecedented positive trend

Supporting Information:

Supporting Information may be found in the online version of this article.

Correspondence to:
K. E. King, kking@utk.edu

Citation:
King, K. E., Harley, G. L., Maxwell, J. T., Rayback, S., Cook, E., Maxwell, R. S., et al. (2024). Reconstructed late summer maximum temperatures for the southeastern United States from tree-ring blue intensity. *Geophysical Research Letters*, *51*, e2024GL109099. https://doi.org/10.1029/2024GL109099

Received 5 MAR 2024
Accepted 18 MAY 2024

Author Contributions:

Conceptualization: Grant L. Harley, Justin T. Maxwell, Shelly Rayback
Data curation: Grant L. Harley, Edward Cook, R. Stockton Maxwell, Maegen L. Rochner
Funding acquisition: Grant L. Harley,

Reconstructed Late Summer Maximum Temperatures for the Southeastern United States From Tree-Ring Blue Intensity

Karen E. King[1], Grant L. Harley[2], Justin T. Maxwell[3], Shelly Rayback[4], Edward Cook[5], R. Stockton Maxwell[6], Maegen L. Rochner[7], Ellen V. Bergan[2], Zachary Foley[8], Matthew Therrell[8], and Joshua Bregy[9]

Department of Geography and Sustainability, University of Tennessee Knoxville, Knoxville, TN, USA, Department of Earth and Spatial Sciences, University of Idaho, Moscow, ID, USA, [3]Department of Geography, Indiana University, Bloomington, IN, USA, [4]Department of Geography and Geosciences, University of Vermont, Burlington, VT, USA, [5]Tree Ring Lab, Lamont-Doherty Earth Observatory, Palisades, NY, USA, [6]Department of Geospatial Science, Radford University, Radford, VA, USA, [7]Department of Geographic and Environmental Sciences, University of Louisville, Louisville, KY, USA, [8]Department of Geography, University of Alabama, Tuscaloosa, AL, USA, [9]Department of Environmental Engineering and Earth Sciences, Clemson University, Anderson, SC, USA

Abstract Over recent decades, the southeastern United States (Southeast) has become increasingly well represented by the terrestrial climate proxy record. However, while the paleo proxy records capture the region's hydroclimatic history over the last several centuries, the understanding of near surface air temperature variability is confined to the comparatively shorter observational period (1895-present). Here, we detail the application of blue intensity (BI) methods on a network of tree-ring collections and examine their utility for producing robust paleotemperature estimates. Results indicate that maximum latewood BI (LWBI) chronologies exhibit positive and temporally stable correlations (r = 0.28–0.54, p < 0.01) with summer maximum temperatures. As such, we use a network of LWBI chronologies to reconstruct August-September average maximum temperatures for the Southeast spanning the period 1760–2010 CE. Our work demonstrates the utility of applying novel dendrochronological techniques to improve the understanding of the multicentennial temperature history of the Southeast.

1. Introduction

While anthropogenic climate change has global-scale implications, an improved understanding of its regionalscale manifestations is extremely relevant for community planning and resource management. Despite 20th century increases to the global-scale anthropogenic warming signal, observed summer maximum temperatures across the southeastern United States (hereafter, Southeast) do not reflect steadily increasing positive trends over the last century (Eischeid et al., 2023). Colloquially termed the "warming hole," this phenomenon has spurred major research efforts linking the lack of increased summer warming to short-wave cloud forcing due to aerosols (Mascioli et al., 2017; Yu et al., 2014), trends in land cover change (e.g., reforestation; Barnes et al., 2024), and interactions between temperature and changing precipitation regimes (Eischeid et al., 2023). As evidence currently supports numerous explanations for the Southeast "warming hole," contextualizing this phenomenon prior to the observational record using proxy data is critical for improving the understanding of its underlying mechanisms. Many regions of North America contain dense networks of paleo proxy data (e.g., Rouston et al., 2020; Guitermann et al., 2023), which can provide regional estimates of past climatic variability spanning

Plain Language Summary Tree-ring data are important sources of paleoclimate information, which allow for the longer-term evaluation of modern climate values and trends. Compared to much of North America, the Southeastern United States (Southeast) contains substantially fewer paleoclimate records from tree rings, and no estimates of past temperature variability which extend before the observational period. Employing a recently developed technique, which uses light reflectance properties of wood to obtain a representative metric of tree-ring density, we develop a network of temperature-sensitive tree-ring records across the Southeast. These records enable us to reconstruct late summer maximum temperatures across the region spanning the period 1760–2023 CE. As few ground-based, pre-instrumental temperature records previously existed for this region, our reconstruction allows for an improved understanding of the region's multi-centennial climatic history.

Project administration: Grant L. Harley, Justin T. Maxwell, Shelly Rayback
Resources: Grant L. Harley, Justin T. Maxwell, Shelly Rayback, Edward Cook, R. Stockton Maxwell, Maegen L. Rochner, Ellen V. Bergan, Zachary Foley, Matthew Therrell, Joshua Bregy
Software: Edward Cook
Writing – review & editing: Grant L. Harley, Justin T. Maxwell, Shelly Rayback, Edward Cook, R. Stockton Maxwell, Maegen L. Rochner, Ellen V. Bergan, Zachary Foley, Matthew Therrell, Joshua Bregy

the last several centuries to millennia (e.g., Marlon et al., 2017), and more specifically, can highlight past climate analogs for comparison with modern conditions. For example, sediment core records from the southern Appalachian Mountains indicate that the Southeast warmed concurrently with much of North America during an analogously warm period during the mid-Holocene, thereby suggesting that the 20th century "warming hole" is anomalous in time (Tanner et al., 2015). However, as very few high-resolution paleotemperature records currently exist for the Southeast, continued efforts to derive pre-observational temperature estimates from proxy data would be advantageous for further improving the understanding of the "warming hole" and regional system responses to climate change.

Compared to other regions in North America, the relative paucity of temperature proxy records from tree rings in the Southeast is partially attributed to increasing difficulty locating trees growing in energy-limited environments at lower latitudes. Moreover, with decreasing latitude, moisture sensitivity frequently dominates the climatic signal embedded in radial tree growth (Martin-Benito & Pederson, 2015). In the closed-canopy forests of the Southeast, ecological factors such as canopy dynamics, insect infestation, and anthropogenic logging practices can also heavily impact radial growth. However, in recent decades, methodological advances with densiometric growth parameters such as maximum ring density (MXD; Schweingruber et al., 1978) and blue intensity (BI; McCarroll et al., 2002) have substantially increased the number of temperature sensitive tree-ring records at increasingly lower latitudes in North America, where total-ring width (TRW) historically has been less successful (Briffa et al., 1992, 1994; Heeter et al., 2020, 2021; King et al., 2024). Due to the relative affordability and accessibility of BI methods, they have been widely adopted by the global tree-ring community in recent decades (Kaczka & Wilson, 2021).

As the application of BI methods continues to expand, recent studies have explored the suitability of using BI parameters from *Picea rubens* Sarg. (red spruce) and *Tsuga candensis* (L.) Carrière (eastern hemlock) in the midlatitudes of the eastern US to develop temperature sensitive tree-ring records (Harley et al., 2021; Heeter et al., 2019). Here, we expand upon the original tree-ring network first described by Harley et al. (2021) by developing and evaluating the climate signal of 12 maximum latewood BI (LWBI) chronologies from the southern Appalachian Mountain region of the eastern US. Further, we use this network of chronologies to develop the first reported temperature reconstruction for the Southeast using tree-ring data.

2. Materials and Methods

2.1. Developing a Network of LWBI Chronologies Across the Southeast

The tree-ring data in this study (Figure 1; Table S1 in Supporting Information S1) are derived from a combination of recently sampled sites and preexisting tree-ring collections, which were reprocessed for BI methods. The treering data are comprised of two species: *P. rubens* and *T. canadensis*. Within the Southeast, the distribution of *P. rubens* is limited to high-elevation (>1500 m) disjunct populations, with limited occurrences of isolated, lowland bog populations (Adams et al., 2012). As such, except for one location in the network (ACS site), all *P. rubens* samples were collected from high-elevation locations at the southern range periphery (Little & Viereck, 1971; Figure 1). In the southern Appalachian Mountains, small, isolated populations of *T. canadensis* are restricted to cool, moist slopes with north to east aspects and low to middle slope positions at the southern range periphery (Hart & Shankman, 2005). As hemlock wooly adelgid (*Adelges tsugae* Annand, HWA; McClure, 1996; Vose et al., 2013) is one of the most pervasive threats to *T. canadensis*, we restricted sampling for new collections to stands with known HWA treatments. For each new collection, we sampled between 15 and 20 trees, taking two cores per tree with handheld increment borers. New samples were mounted and dried for 24 hr. Both new and existing collections were incrementally shaved using a core microtome to achieve a flat surface and a clear radial view of annual growth bands (Gärtner & Nievergelt, 2010). All samples were then scanned on an Epson 12000XL scanner at 3200 dpi resolution using the Silverfast AI Plus software, calibrated with IT8 calibration. For each site collection, samples were first visually cross dated. We delineated annual ring boundaries and measured TRW using the software CooRecorder (Larsson, 2014), then statistically validated the visual cross dating of the TRW series using the program COFECHA (Holmes, 1983). After each sample was absolutely dated, we then collected LWBI in CooRecorder (Heeter et al., 2022). All site-level LWBI chronologies

were detrended using a variety of frameworks and splines (Table S1 in Supporting Information S1) in order to minimize non-climatic trends in the data using both the dplR package (Bunn, 2008) and the RCSigFree program (Melvin & Briffa, 2008; https://www. ldeo.columbia.edu/tree-ring-laboratory/resources/software).

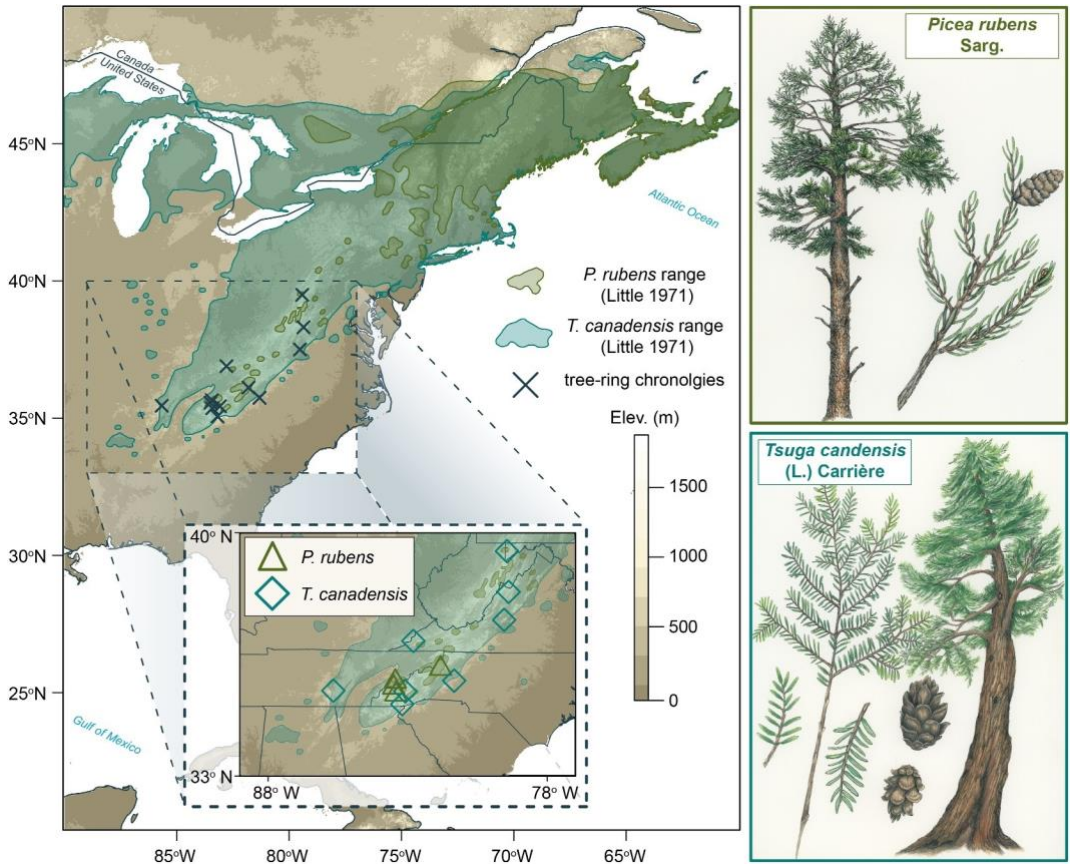

Figure 1. Locations of the 12 site-level LWBI chronologies examined for climate response (*left panel*). The network is comprised of two species, *Picea rubens* Sarg. and *Tsuga canadensis* (L.) Carriere situated near the southern range periphery of each species. Right-side panels are original author illustrations.

2.2. Evaluating Climate-Growth Relationships Across the Tree-Ring Network

To examine the relationship between the site-level LWBI chronologies and their local climate, we used a suite of monthly average climate variables from the 0.5° gridded CRU TS 4.07 land data set (Harris et al., 2020). For each site, we compiled monthly precipitation (Pcp), self-calibrating Palmer's Drought Severity Index (scPDSI), and mean (T_{mean}) and maximum (T_{max}) temperature data from the nearest 0.5° CRU grid cell. We assessed the strength of the relationship of each site-level LWBI chronology and each local climate variable using a Pearson's correlation over the shared period by the instrumental and all tree-ring data (1901–1980 CE). For the temperature variables, we examined the climate-growth correlations over varying, multi-month seasonal windows to determine the potential optimal season for reconstruction. To assess the temporal stability of the climate-growth relationships, we applied dynamic regression modeling between the LWBI chronologies and the instrumental variables using a Kalman filter (Harvey, 1990). To determine if the dynamic regression model provided a better fit to the data compared to a constant-coefficient model, we used the modified Akaike Information Criteria (AIC) (Hurvich & Tsai, 1989), where the AIC of the dynamic model (AIC_{td}) must be smaller than the AIC value of the constant coefficient model (AIC_{cm}) by at least 2 (AIC_{td}–AIC_{cm} < 2; Jones, 1985). We used these climate signal strength and stability screenings to identify candidate predictors from the site-level LWBI chronologies for the reconstruction.

2.3. Reconstructing Past Temperature Variability With Tree-Ring LWBI

We used principal components analysis (PCA) to identify the dominant climatic signals embedded across the candidate tree-ring predictors which passed initial climate signal screenings. To determine the spatial footprint of the instrumental reconstruction target, we ran a spatial Pearson's correlation between the leading principal component of the tree-ring data (PC1) and the gridded seasonal target data. Based on these results, we then calculated a regional average instrumental target using CRU data from all grid points where $r \geq 0.6$ ($p < 0.01$). Once the regional instrumental target was identified, we used a nested principal component regression approach (Cook et al., 1999) to reconstruct surface air temperatures. For the common period nest, we calibrated and validated the reconstruction over the period 1901–1980 CE and used a split calibration/verification approach, calibrating over the period 1941–1980 CE and verifying over the period 1901–1940 CE. We repeated the approach for the two forward nests, 1901–1998 CE and 1901–2010 CE, where the verification period remained constant, but the calibration period varied according to end year of each nest (e.g., 1941–2010 CE). We evaluated the reconstruction goodness-of-fit using two calibration statistics: the coefficient of determination (CRSQ or R^2) and the cross-validation leave-one-out reduction of error (CVRE) statistic. Reconstruction accuracy was determined for the validation period of withheld data using the explained variance (VRSQ), reduction of error (VRE), and coefficient of efficiency (VCE) statistics, where high values of VRSQ and positive values of VRE, and VCE values indicate good model skill (Cook et al., 1994, 1999). After final calibration and validation, we then biascorrected the reconstruction using a quantile mapping approach based on localized linear regression (Robeson et al., 2020) and augmented the reconstruction ending in 2010 CE with instrumental data spanning 2011–2023 CE. We quantified reconstruction uncertainty using the root mean squared error (RMSE).

3. Results and Discussion

3.1. Signal-Strength and Stability of Climate-Growth Relationships

Across the network, climate-growth responses suggest that warm season temperature is the dominant driver of year-to-year latewood densiometric growth variability and show no indication of interacting climatic controls (Figure 2). Overall, the LWBI chronologies show slightly stronger positive correlations with T_{max} than with T_{mean}, particularly during August and September. Results document substantial variation in the onset of positive temperature response during the spring season (March-May response), whereas the late summer seasonal response (August–September; AS) is more consistent. For months where LWBI shows positive, significant correlations ($p < 0.01$) with T_{max}, LWBI concurrently shows negative correlations with both Pcp and scPDSI. However, the relationships between the LWBI chronologies and temperature are typically stronger than with the hydroclimate variables. The inverse relationship between LWBI and temperature versus LWBI and both Pcp and scPDSI is especially apparent over the late summer. This pattern is not surprising given the negative relationship between AS T_{max} and AS Pcp in the local CRU data ($r = -0.46$, $p < 0.01$, 1901–2022 CE) and further reflects the ability of the LWBI data to capture this aspect of the region's climate system. By comparing the network-wide response to T_{max} over varying seasonal windows, we determine that the AS window results in the strongest positive correlations with the temperature variables across the LWBI network. Three of the 12 site-level chronologies (ACS, GFM, and KTH sites) show no significant ($p < 0.01$) correlations with either AS T_{max} or T_{mean}, and one chronology (SG site) shows a weakly negative, but still significant correlation with AS T_{max}. As such, these four chronologies are excluded as candidate predictors for the reconstruction.

For the eight LWBI chronologies that exhibit significant ($p < 0.01$), positive correlations with their local AS T_{max} data, we use dynamic regression modeling to evaluate the temporal stability of the climate-growth relationships over the shared period (1901–1980 CE). Apart from the HCH site chronology, the constant coefficient model explains a higher proportion of the relationship explained variance than the time-dependent dynamic model at each site, thereby indicating relative temporal stability of the climate growth relationships (Figure S2 in Supporting Information S1). Regression coefficients for the HCH site indicate a stronger relationship between the LWBI data and AS T_{max} in the latter half of the observational record (*ca*. 1940–1980) than in the earlier half.

Due to the instability of the temperature response, the HCH chronology is also excluded from the subsequent analysis and the reconstruction predictor pool. The non-ubiquitous temperature response (strength and stability) of LWBI chronologies across the Southeast network is somewhat consistent with previous work, which documents the heterogeneous climatic response from TRW series of high elevation *P. rubens* across the southern Appalachian range (Rochner et al., 2023).

While BI parameters have been previously shown to be less affected by disturbance agents than traditional radial growth parameters (Jiang et al., 2022), we suspect that the combination of microsite conditions (e.g., elevation, slope position, substrate) and regional variation in the response of *P. rubens* and *T. canadensis* stands to exogenous disturbance regimes, influences the suitability of each site-level chronology as a candidate predictor for the

10.1029/2024GL109099

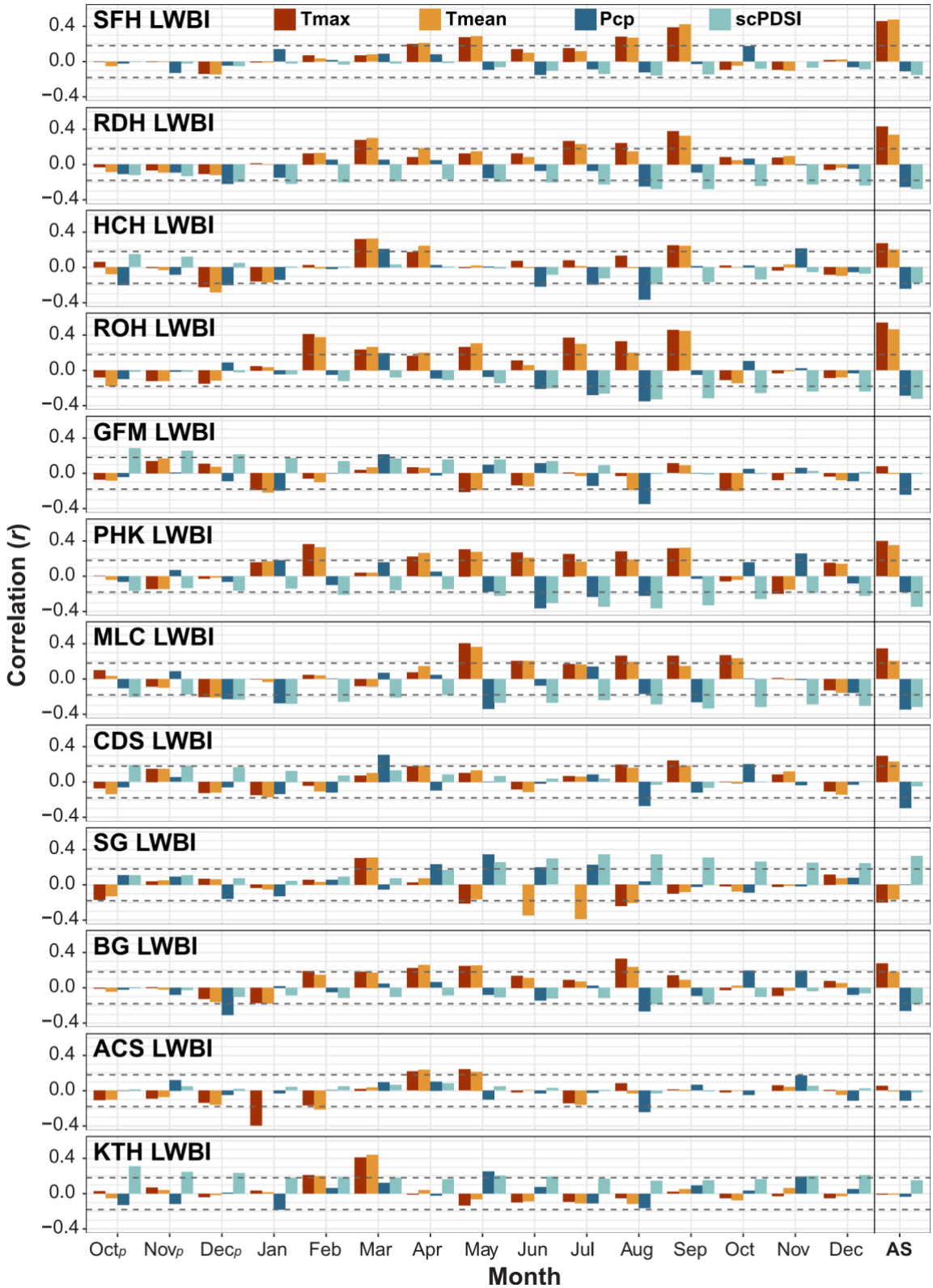

Figure 2. Pearson's correlations (*r*-value) between all site-level LWBI chronologies and their local climate data, calculated over the common period 1901–1980 CE. Climate variables: maximum temperature (T_{max}), mean temperature (T_{mean}), precipitation (Pcp) and self-calibrating Palmer's Drought Severity Index (scPDSI) are sourced from the CRU TS land 4.07 data set within 0.5° of each chronology site. Dashed horizontal lines indicate significance at the $p < 0.01$ level.

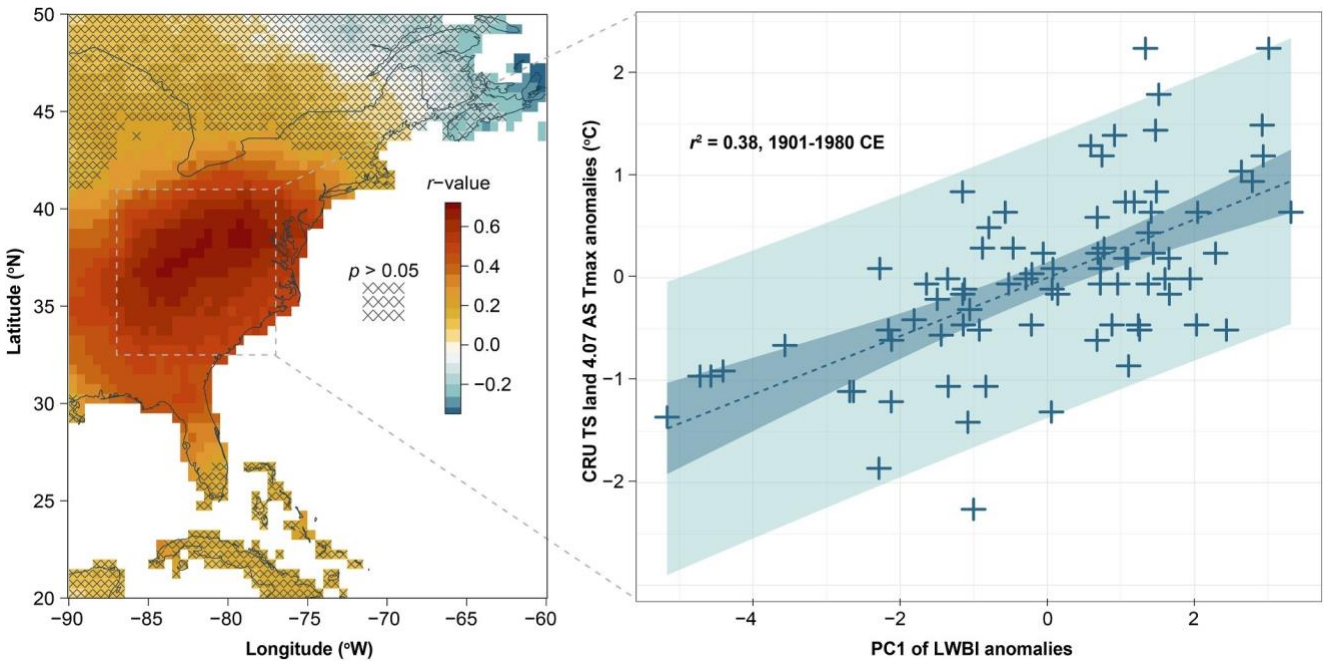

Figure 3. Spatial Pearson's correlation (*r*-value) between the leading principal component of latewood blue intensity (PC1 of LWBI) and CRU TS land 4.07 AugustSeptember average maximum temperature (AS T_{max}) (*left panel*). The dashed gray box indicates the region over which the instrumental AS T_{max} data are averaged for the reconstruction model. Based on a linear regression model, PC1 of LWBI explains 38% of regionally averaged AS T_{max} over the common period 1901–1980 CE (*right panel*). The linear model is plotted with 95% confidence (dark blue shading) and prediction intervals (light blue shading). Anomalies are relative to the 1901–1980 CE mean.

temperature reconstruction. For example, despite the GFM *P. rubens* collection having a similar elevation and slope position as the CDS *P. rubens* collection, the GFM LWBI chronology shows significant, negative correlation with August Pcp, thereby indicating that local summer moisture availability is a more dominant limiting factor than maximum temperatures at this site. Exogenous disturbance regimes also play an important role in the growth dynamics of the closed-canopy forests across the Southeast. For example, the impact of acid deposition on *P. rubens* is well documented in the northeastern United States, where tree-ring data reflect substantial declines in radial growth in the 1960s (Cook & Zedaker, 1992), followed by more recent recovery (Kosiba et al., 2018; Mathias & Thomas, 2018). However, tree-ring data provide less conclusive evidence of ubiquitous growth decline or changes in climate sensitivity of the species due to acid deposition in the Southeast (Cook, 1988). In this study, neither the LWBI chronologies from the CDS or MLC sites indicate weakening climate-growth relationships in the latter 20th century. While previous work demonstrates negative relationships between radial growth of *P. rubens* and SO_2 and NO_X emissions (Rochner et al., 2023; Soulé, 2011), determining the influence of acid deposition on densiometric growth of *P. rubens* requires further investigation. Similarly, disturbance from HWA may be influencing the climate sensitivity of several of the LWBI chronologies in recent decades. For example, despite annual treatments, the KTH site shows growth reductions associated with known infestations of HWA within the last several decades (Brown, 2004; Figure S1 in Supporting Information S1). While the impact of HWA on the influence of densiometric wood growth has not been widely studied, Walker et al. (2014) indicate that across the species range, both mean latewood cell wall thickness and radial cell diameter of *T. canadensis* are significantly reduced ($p < 0.001$) in years following HWA infestation. Given these findings, the four *T. canadensis* LWBI chronologies which pass our initial climate screenings (SFH, ROH, PHK, and BG) are evaluated for growth reductions coinciding with HWA outbreak years and truncated prior to subsequent analysis (Table S1 in Supporting Information S1).

3.2. PCA Results

We apply a PCA to seven LWBI chronologies that pass the initial climate signal strength and stability screenings. PC1 explains 38% of the total variance across the network chronologies. The PC1 time series shows strong, positive correlation with AS T_{max} spatially (Figure 3). Using the criteria where $r \geq 0.6$ ($p < 0.01$) between PC1

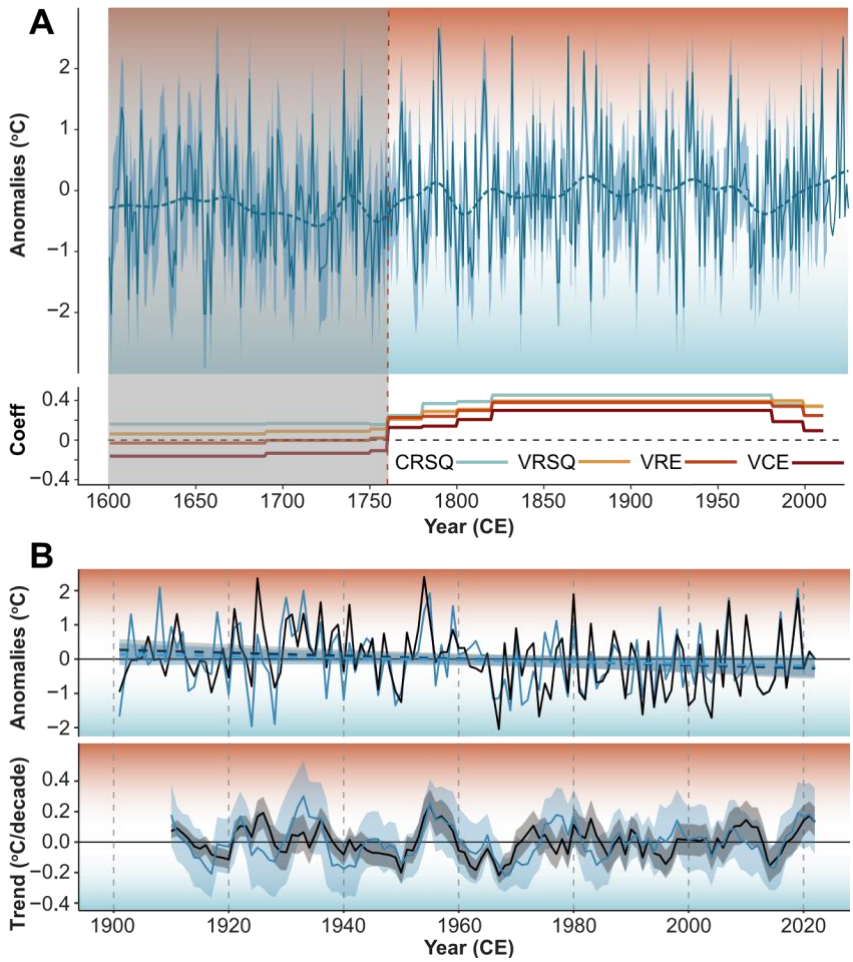

Figure 4. (a) Reconstructed regional August-September average maximum temperatures (AS T_{max}) over the period 1600–2022 CE (*top panel*). Annual reconstruction estimates (thin blue lines) are plotted with ±1 root mean squared error (RMSE; blue shading). Multidecadal trends are visualized by smoothing annual estimates with a 30-year low pass filter (thick, blue dashed line). Reconstruction statistics are plotted back to 1600 CE (*bottom panel*). (b) Instrumental (solid, dark brown line) and reconstructed (solid blue line) regional AS T_{max} over the period 1901–2022 CE (*top panel*). Linear trend lines are plotted with 95% confidence intervals (dashed lines with shading). The centennial trends based on reconstruction estimates and instrumental have intercepts of − 0.003 and − 0.004, adjusted r^2 values of 0.004 and 0.02, and *p*-values of 0.22 and 0.05, respectively. Decadal trends (*bottom panel*) in the instrumental (brown line) and reconstruction (blue line) data sets are calculated using a least square regression approach and plotted with 95% confidence intervals (shading). Anomalies are relative to the 1901–1980 CE mean.

and CRU AS T_{max}, we compile a regionally averaged temperature target that comprehensively covers the southern Appalachian Mountain range. PC1 of LWBI data explains 38% of the variation of the regionalized AS T_{max} data over the period 1901–1980 CE.

3.3. Reconstructing Late Summer Maximum Temperature

Using the seven LWBI chronologies as predictors, we skillfully reconstruct AS T_{max} over the Southeast back to 1760 CE (Figure 4a). While the temporal coverage of the tree-ring data spans 1600–2010 CE, negative RE and CE statistics prior to 1760 CE indicate decreased reconstruction skill, and thus, the earliest part of the reconstruction should be interpreted with caution for subsequent analysis. Over the common period nest (1820–1980 CE), the reconstruction model has an explained variance of 45.3% over the calibration period and 40.5% over the verification period. The explained variance of the calibration and verification periods decreases as the number of chronologies comprising each backward nest decreases through time, yet the 1780–1819 CE nest still has a calibration period $r^2 > 0.36$ and a verification period $r^2 > 0.28$. The RMSE ranges from 0.835 to 0.712, with the lowest uncertainty occurring over the 1820–1980 CE common period nest. Multidecadal smoothing indicates slight cooling prior to 1860 CE, however, the cooling trend becomes much more pronounced over the period 1600–1780 CE. As the pre-1760 CE portion of the reconstruction should be interpreted with caution, additional sampling is needed to improve the fidelity of the reconstruction over this earlier period. Moreover, the future improved chronologies should be reevaluated for the preservation of multi-centennial variability, which in turn, would contribute to a more accurate evaluation of the potential long-term cooling and the expression of the Little Ice Age in the Southeast. While the current network of LWBI chronologies shows the potential to extend the reconstruction back in time to at least 1600 CE, the complex land-use and settlement history of the Southeast often presents challenges to obtaining old-age trees required to extend paleoclimatic estimates further back in time. However, targeting long-lived species whose potential for BI methods is currently unexplored (e.g., bald cypress; *Taxodium distichum* L.), as well as investigating paleoclimatic signals in archeological material (e.g., Bregy et al., 2022; DeGraauw et al., 2024), may be several strategies to overcome this perceived temporal limitation in the region.

The reconstruction estimates track the CRU instrumental data with relative skill and reflect similar decadal trends (Figure 4b; $r = 0.55$, $p < 0.01$) to those shown in the CRU data over the observational period (1901–2022 CE). However, the reconstruction slightly underestimates cooling in both the earliest and latest parts of the shared observational period and overestimates warming trends in the 1930s and 1970s. While there is strong coherence between the decadal warming and cooling trends observed in both the CRU and reconstructed data, neither reflect the statistically significant ($p < 0.05$) centennial warming trends similar to those documented across other regions of the US (Eischeid et al., 2023; Figure S3 in Supporting Information S1) and globally (Arias et al., 2021) over the last century. Rather, multi-decadal cooling occurs from the mid-1950s into the mid-1970s. Temperatures then trend positively over the 1970s, plateau, and then again from the 1990s to present. One hypothesis suggests that the existence of the Southeast "warming hole" is partially due to aerosols, which can have a negative indirect effect on maximum temperatures in situations where cloud formation increases (Stevens & Feingold, 2009). Indeed, both CRU and reconstructed T_{max} values for the Southeast show significant relationships ($p < 0.001$) with regional cloud coverage over the last century (Figure S4 in Supporting Information S1). Notably, both anthropogenic and natural biogenic sources of volatile organic compound emissions have previously been linked to regional summer cooling in the Southeast (Goldstein et al., 2009). Despite the multi-decadal persistence of the "warming hole" across much of the 20th century, summer maximum temperatures have trended positively since the 1990s. This increasing trend is likely due to a combination of simultaneous reductions in anthropogenic aerosols following the Clean Air Act Amendments of 1989–1990 and increases in greenhouse gases. As such, a failure to reduce greenhouse gas emissions in the coming decades, coupled with projected reductions in aerosol emissions may lead to a decline in future multidecadal periods of regional summer cooling (Mascioli et al., 2017). Recent work suggests that the persistence of the Southeast warming hole over the last two decades, despite accelerated global warming, is consistent with 21st century trends in increasing regional summer rainfall (Eischeid et al., 2023). Moreover, current projections point to an intensification of the hydrologic cycle over the

Southeast in the coming decades (Akinsanola et al., 2020; Li et al., 2013). If, in fact, the maintenance of the Southeast warming hole is becoming less regulated by aerosols and increasingly tied to summer rainfall, using a combination of paleorecords to achieve a longer-term understanding of the relationship between changes to

the hydrologic cycle and summer temperatures may provide critical insights into future extreme heat-related risk for the Southeast.

4. Conclusions

We demonstrate the application of BI methods across a network of conifers to provide a tree-ring-based temperature reconstruction for the Southeast, which allows for the multi-century contextualization of modern values and trends. Notably, the 20th–21st centuries across the Southeast are not characterized by steadily increasing latesummer maximum temperatures, as is documented across much of North America and globally. While substantial uncertainty remains regarding the relationship between projected hydroclimatic shifts under anthropogenic warming scenarios and the future persistence of the Southeast "warming hole," the paleoclimate record may provide important insights into future temperature-hydroclimate interactions. Although BI methods have immense potential to expand the current representation of North America by paleotemperature proxy record, numerous caveats require additional consideration prior to their wide-spread employment in the closed canopy forests of the Southeast. Although perhaps to a lesser degree than with radial growth metrics, both microsite

conditions and exogenous disturbance regimes from defoliators likely still influence the suitability of LWBI chronologies as candidate predictors for climate reconstruction. As LWBI is closely linked to latewood cell geometry (ratio of cell wall area to cell lumen area; Björklund et al., 2021), future efforts comparing BI methods and quantitative wood anatomy (Von Arx et al., 2016) would be highly beneficial for evaluating the influence of defoliator-type disturbances on densiometric tree growth.

Conflict of Interest

The authors declare no conflicts of interest relevant to this study.

Data Availability Statement

All tree-ring data and the temperature reconstruction are available in the in-text data citation reference: King (2024).

Acknowledgments

This project was financially supported by the National Science Foundation P2C2 Program: AGS-2002524, AGS-2102888, AGS-2002494, AGS-1805276, AGS1805617, and the University of Alabama ASSURE Grant. We thank all field and laboratory assistance for their efforts towards the completion of this project.

References

Adams, M. B., Cogbill, C., Cook, E. R., DeHayes, D. H., Fernandez, I. J., Jensen, K. F., et al. (2012). In *Ecology and decline of red spruce in the eastern United States* (Vol. 96). Springer Science & Business Media.

Akinsanola, A. A., Kooperman, G. J., Reed, K. A., Pendergrass, A. G., & Hannah, W. M. (2020). Projected changes in seasonal precipitation extremes over the United States in CMIP6 simulations. *Environmental Research Letters*, *15*(10), 104078. https://doi.org/10.1088/1748-9326/abb397

Arias, P., Bellouin, N., Coppola, E., Jones, R., Krinner, G., Marotzke, J., et al. (2021). Climate change 2021: The physical science basis. In *Contribution of Working Group I to the Sixth Assessment Report of the Intergovernmental Panel on Climate Change; Technical Summary*.

Barnes, M. L., Zhang, Q., Robeson, S. M., Young, L., Burakowski, E. A., Oishi, A. C., et al. (2024). A century of reforestation reduced anthropogenic warming in the Eastern United States. *Earth's Future*, *12*(2), e2023EF003663. https://doi.org/10.1029/2023ef003663

Björklund, J., Fonti, M. V., Fonti, P., Van den Bulcke, J., & von Arx, G. (2021). Cell wall dimensions reign supreme: Cell wall composition is irrelevant for the temperature signal of latewood density/blue intensity in Scots pine. *Dendrochronologia*, *65*, 125785. https://doi.org/10.1016/ j.dendro.2020.125785

Bregy, J. C., Maxwell, J. T., Robeson, S. M., Harley, G. L., Elliott, E. A., & Heeter, K. J. (2022). US Gulf Coast tropical cyclone precipitation influenced by volcanism and the North Atlantic subtropical high. *Communications Earth & Environment*, *3*(1), 164. https://doi.org/10.1038/ s43247-022-00494-7

Briffa, K. R., Jones, P. D., & Schweingruber, F. H. (1992). Tree-ring density reconstructions of summer temperature patterns across western North America since 1600. *Journal of Climate*, *5*(7), 735–754. https://doi.org/10.1175/1520-0442(1992)005<0735:trdros>2.0.co;2

Briffa, K. R., Jones, P. D., & Schweingruber, F. H. (1994). Summer temperatures across northern North America: Regional reconstructions from 1760 using tree-ring densities. *Journal of Geophysical Research*, *99*(D12), 25835–25844.

Brown, J. (2004). Impacts of hemlock woolly adelgid on Canadian and Carolina hemlock forests. In *Proceedings: Land use change and implications for biodiversity on the Highlands plateau: A report by the Carolina Environmental Program, Part A* (pp. 19–36). Highlands Biological Station.

Bunn, A. G. (2008). A dendrochronology program library in R (dplR). *Dendrochronologia*, *26*(2), 115–124. https://doi.org/10.1016/j.dendro.2008.01.002

Cook, E. R. (1988). A tree ring analysis of red spruce in the southern Appalachian Mountains. In *Forest Service general technical report SOUnited States*. Southern Forest Experiment Station (USA).

Cook, E. R., Briffa, K. R., & Jones, P. D. (1994). Spatial regression methods in dendroclimatology: A review and comparison of two techniques. *International Journal of Climatology*, *14*(4), 379–402. https://doi.org/10.1002/joc.3370140404

Cook, E. R., Meko, D. M., Stahle, D. W., & Cleaveland, M. K. (1999). Drought reconstructions for the continental United States. *Journal of Climate*, *12*(4), 1145–1162. https://doi.org/10.1175/1520-0442(1999)012<1145:drftcu>2.0.co;2

Cook, E. R., & Zedaker, S. M. (1992). The dendroecology of red spruce decline. In *Ecology and decline of red spruce in the eastern United States* (pp. 192–231). Springer New York.

de Graauw, K., Rochner, M., van de Gevel, S., Stachowiak, L., Collins-Key, S., Henderson, J., et al. (2024). Comparing the impact of live-tree versus historic-timber data on palaeoenvironmental inferences in tree-ring science, eastern North America. *The Holocene*, *34*(1), 3–13. https://doi.org/10.1177/09596836231200437

Eischeid, J. K., Hoerling, M. P., Quan, X. W., Kumar, A., Barsugli, J., Labe, Z. M., et al. (2023). Why has the summertime Central US warming hole not disappeared? *Journal of Climate*, *36*(20), 7319–7336. https://doi.org/10.1175/jcli-d-22-0716.1

Gärtner, H., & Nievergelt, D. (2010). The core-microtome: A new tool for surface preparation on cores and time series analysis of varying cell parameters. *Dendrochronologia*, *28*(2), 85–92. https://doi.org/10.1016/j.dendro.2009.09.002

Goldstein, A. H., Koven, C. D., Heald, C. L., & Fung, I. Y. (2009). Biogenic carbon and anthropogenic pollutants combine to form a cooling haze over the southeastern United States. *Proceedings of the National Academy of Sciences*, *106*(22), 8835–8840. https://doi.org/10.1073/pnas.0904128106

Guiterman, C. H., Gille, E., Shepherd, E., McNeill, S., Payne, C. R., & Morrill, C. (2023). The international tree-ring data bank at fifty: Status of stewardship for future scientific discovery. *Tree-Ring Research*, *80*(1). https://doi.org/10.3959/trr2023-2

Harley, G. L., Heeter, K. J., Maxwell, J. T., Rayback, S. A., Maxwell, R. S., Reinemann, T. E., & H Taylor, A. (2021). Towards broad-scale temperature reconstructions for Eastern North America using blue light intensity from tree rings. *International Journal of Climatology*, *41*(S1), E3142–E3159. https://doi.org/10.1002/joc.6910

Harris, I., Osborn, T. J., Jones, P., & Lister, D. (2020). Version 4 of the CRU TS monthly high-resolution gridded multivariate climate dataset. *Scientific Data*, *7*(1), 109. https://doi.org/10.1038/s41597-020-0453-3

Hart, J. L., & Shankman, D. (2005). Disjunct eastern hemlock (Tsuga canadensis) stands at its southern range boundary1. *Journal of the Torrey Botanical Society*, *132*(4), 602–612. https://doi.org/10.3159/1095-5674(2005)132[602:dehtcs]2.0.co;2

Harvey, A. C. (1990). Forecasting, structural time series models and the Kalman filter.

Heeter, K. J., Harley, G., Maxwell, J. T., McGee, J. H., & Matheus, T. J. (2020). Late summer temperature variability for the Southern Rocky Mountains (USA) since 1735 CE: Applying blue light intensity to low-latitude Picea engelmannii Parry ex Engelm. *Climatic Change*, *162*(2), 965–988. https://doi.org/10.1007/s10584-020-02772-9

Heeter, K. J., Harley, G. L., Maxwell, J. T., Wilson, R. J., Abatzoglou, J. T., Rayback, S. A., et al. (2021). Summer temperature variability since 1730 CE across the low-to-mid latitudes of western North America from a tree ring blue intensity network. *Quaternary Science Reviews*, *267*, 107064. https://doi.org/10.1016/j.quascirev.2021.107064

Heeter, K. J., Harley, G. L., Van De Gevel, S. L., & White, P. B. (2019). Blue intensity as a temperature proxy in the eastern United States: A pilot study from a southern disjunct population of Picea rubens (Sarg.). *Dendrochronologia*, *55*, 105–109. https://doi.org/10.1016/j.dendro.2019.04.010

Heeter, K. J., King, D. J., Harley, G. L., & Kaczka, R. J. (2022). Video tutorial: Measuring blue intensity with the CooRecorder software application. *Dendrochronologia*, *76*, 125999. https://doi.org/10.1016/j.dendro.2022.125999

Holmes, R. L. (1983). Computer-assisted quality control in tree-ring dating and measurement.

Hurvich, C. M., & Tsai, C. L. (1989). Regression and time series model selection in small samples. *Biometrika*, *76*(2), 297–307. https://doi.org/10.1093/biomet/76.2.297

Jiang, Y., Begović, K., Nogueira, J., Schurman, J. S., Svoboda, M., & Rydval, M. (2022). Impact of disturbance signatures on tree-ring width and blue intensity chronology structure and climatic signals in Carpathian Norway spruce. *Agricultural and Forest Meteorology*, *327*, 109236. https://doi.org/10.1016/j.agrformet.2022.109236

Jones, R. H. (1985). Time series analysis- time Domain. In A. H. Murphy & R. W. Katz (Eds.), *Probability, statistics, and decision making in the atmospheric sciences* (pp. 223–259). Westview Press.

Kaczka, R. J., & Wilson, R. (2021). I-BIND: International Blue intensity network development working group. *Dendrochronologia*, *68*, 125859. https://doi.org/10.1016/j.dendro.2021.125859

King, K. E. (2024). August-September maximum temperature reconstruction for the Southeastern United States (1760-2022 CE) [Dataset]. *Dryad*. https://doi.org/10.5061/dryad.mpg4f4r76

King, K. E., Cook, E. R., Anchukaitis, K. J., Cook, B. I., Smerdon, J. E., Seager, R., et al. (2024). Increasing prevalence of hot drought across western North America since the 16th century. *Science Advances*, *10*(4), eadj4289. https://doi.org/10.1126/sciadv.adj4289

Kosiba, A. M., Schaberg, P. G., Rayback, S. A., & Hawley, G. J. (2018). The surprising recovery of red spruce growth shows links to decreased acid deposition and elevated temperature. *Science of the Total Environment*, *637*, 1480–1491. https://doi.org/10.1016/j.scitotenv.2018.05.010

Larsson, L. (2014). CooRecorder and Cdendro programs of the CooRecorder/Cdendro package version, 7.

Li, L., Li, W., & Deng, Y. (2013). Summer rainfall variability over the Southeastern United States and its intensification in the 21st century as assessed by CMIP5 models. *Journal of Geophysical Research: Atmospheres*, *118*(2), 340–354. https://doi.org/10.1002/jgrd.50136

Little, E. L., & Viereck, L. A. (1971). In *Atlas of United States trees: (no. 1146). Conifers and important hardwoods, by EL Little, Jr* (Vol. 1). US Government Printing Office.

Marlon, J. R., Pederson, N., Nolan, C., Goring, S., Shuman, B., Robertson, A., et al. (2017). Climatic history of the northeastern United States during the past 3000 years. *Climate of the Past*, *13*(10), 1355–1379. https://doi.org/10.5194/cp-13-1355-2017

Martin-Benito, D., & Pederson, N. (2015). Convergence in drought stress, but a divergence of climatic drivers across a latitudinal gradient in a temperate broadleaf forest. *Journal of Biogeography*, *42*(5), 925–937. https://doi.org/10.1111/jbi.12462

Mascioli, N. R., Previdi, M., Fiore, A. M., & Ting, M. (2017). Timing and seasonality of the United States "warming hole". *Environmental Research Letters*, *12*(3), 034008. https://doi.org/10.1088/1748-9326/aa5ef4

Mathias, J. M., & Thomas, R. B. (2018). Disentangling the effects of acidic air pollution, atmospheric CO_2, and climate change on recent growth of red spruce trees in the Central Appalachian Mountains. *Global Change Biology*, *24*(9), 3938–3953. https://doi.org/10.1111/gcb.14273

McCarroll, D., Pettigrew, E., Luckman, A., Guibal, F., & Edouard, J. L. (2002). Blue reflectance provides a surrogate for latewood density of highlatitude pine tree rings. *Arctic Antarctic and Alpine Research*, *34*(4), 450–453. https://doi.org/10.2307/1552203

McClure, M. S. (1996). Hemlock woolly adelgid. *USDA, Forest Service, Forest Health Technology Enterprise Team*, *96*(35).

Melvin, T. M., & Briffa, K. R. (2008). A "signal-free" approach to dendroclimatic standardisation. *Dendrochronologia*, *26*(2), 71–86. https://doi.org/10.1016/j.dendro.2007.12.001

Robeson, S. M., Maxwell, J. T., & Ficklin, D. L. (2020). Bias correction of paleoclimatic reconstructions: A new look at 1,200+ years of Upper Colorado river flow. *Geophysical Research Letters*, *47*(1), e2019GL086689. https://doi.org/10.1029/2019gl086689

Rochner, M. L., Patterson, T. W., Heeter, K. J., & Harley, G. L. (2023). Increased growth synchrony of red spruce in response to acid deposition recovery and climate change across its southern range extent, southeastern USA. *Southeastern Geographer*, *63*(1), 78–97. https://doi.org/10.1353/sgo.2023.0006

Routson, C. C., Kaufman, D. S., McKay, N. P., Erb, M. P., Arcusa, S. H., Brown, K. J., et al. (2020). A multiproxy database of western North American Holocene paleoclimate records. *Earth System Science Data Discussions*, *2020*, 1–39.

Schweingruber, F. H., Fritts, H. C., Bräker, O. U., Drew, L. G., & Schär, E. (1978). The X-ray technique as applied to dendroclimatology.

Soulé, P. T. (2011). Changing climate, atmospheric composition, and radial tree growth in a spruce-fir ecosystem on Grandfather Mountain, North Carolina. *Natural Areas Journal*, *31*(1), 65–74. https://doi.org/10.3375/043.031.0108

Stevens, B., & Feingold, G. (2009). Untangling aerosol effects on clouds and precipitation in a buffered system. *Nature*, *461*(7264), 607–613. https://doi.org/10.1038/nature08281

Tanner, B. R., Lane, C. S., Martin, E. M., Young, R., & Collins, B. (2015). Sedimentary proxy evidence of a mid-Holocene hypsithermal event in the location of a current warming hole, North Carolina, USA. *Quaternary Research*, *83*(2), 315–323. https://doi.org/10.1016/j.yqres.2014.11.004

Von Arx, G., Crivellaro, A., Prendin, A. L., Čufar, K., & Carrer, M. (2016). Quantitative wood anatomy—Practical guidelines. *Frontiers of Plant Science*, *7*, 781. https://doi.org/10.3389/fpls.2016.00781

Vose, J. M., Wear, D. N., Mayfield, A. E., III., & Nelson, C. D. (2013). Hemlock woolly adelgid in the southern Appalachians: Control strategies, ecological impacts, and potential management responses. *Forest Ecology and Management*, *291*, 209–219. https://doi.org/10.1016/j.foreco.2012.11.002

Walker, D. M., Copenheaver, C. A., & Zink-Sharp, A. (2014). Radial growth changes following hemlock woolly adelgid infestation of eastern hemlock. *Annals of Forest Science*, *71*(5), 595–602. https://doi.org/10.1007/s13595-014-0367-3

Yu, S., Alapaty, K., Mathur, R., Pleim, J., Zhang, Y., Nolte, C., et al. (2014). Attribution of the United States "warming hole": Aerosol indirect effect and precipitable water vapor. *Scientific Reports*, *4*(1), 6929. https://doi.org/10.1038/srep06929

Geophysical Research Letters

References From the Supporting Information

Wang, F., Arseneault, D., Boucher, É., Gennaretti, F., Yu, S., & Zhang, T. (2022). Tropical volcanoes synchronize eastern Canada with Northern Hemisphere millennial temperature variability. *Nature Communications*, *13*(1), 5042. https://doi.org/10.1038/s41467-022-32682-6

Wilson, R., Anchukaitis, K., Andreu-Hayles, L., Cook, E., D'Arrigo, R., Davi, N., et al. (2019). Improved dendroclimatic calibration using blue intensity in the southern Yukon. *The Holocene*, *29*(11), 1817–1830. https://doi.org/10.1177/0959683619862037